https://doi.org/10.20965/jrm.2011.p0338

Paper:

Levitation Control of AEROTRAIN: Development of Experimental Wing-in-Ground Effect Vehicle and Stabilization Along *Z* Axis and About Roll and Pitch Axes

Yusuke Sugahara[*1], **Yusuke Ikeuchi**[*1], **Ryo Suzuki**[*2], **Yasuhisa Hirata**[*1], **Kazuhiro Kosuge**[*1], **Yukio Noguchi**[*2], **Satoshi Kikuchi**[*3], **and Yasuaki Kohama**[*4]

[*1]Department of Bioengineering and Robotics, Tohoku University
6-6-01 Aoba, Aramaki, Aoba-ku, Sendai 980-8579, Japan
E-mail: sugahara@irs.mech.tohoku.ac.jp
[*2]Department of Industrial Management and Engineering, Tokyo University of Science
1-3 Kagurazaka, Shinjuku-ku, Tokyo 162-8601, Japan
[*3]Department of Mechanical and Systems Engineering, Gifu University
1-1 Yanagido, Gifu 501-1193, Japan
[*4]New Industry Creation Hatchery Center, Tohoku University
6-6-10 Aoba, Aramaki, Aoba-ku, Sendai 980-8579, Japan
[Received October 1, 2010; accepted February 1, 2011]

The goal of this study is to develop levitation stabilization control for an aerodynamically levitated high-speed, high-efficiency train, "Aero-Train." Levitation occurs due to the wing-in-ground effect acting on a U-shaped guideway. To achieve our goal, we developed a small experimental prototype of the wing-in-ground vehicle, its dynamic model and control for stabilization along the *Z* axis and about the roll and pitch axes using a linear quadratic regulator, as described in this paper. Control effectiveness is confirmed by experimental results.

Keywords: Aero-Train, wing-in-ground effect, levitation control, aerial robotics and mechatronics

1. Introduction

Global environmental problems related to climate change, pollution, and desertification are reportedly due to expanded field, scale, and variety of human activity. The development of high-efficiency transportation technologies is an important task, but on the other hand, there has been a great demand for high-speed systems. Calls are being made for next-generation transportation realizing both of high efficiency and high speed.

Kohama et al. [1–3] proposed a high-efficiency high-speed train system named "Aero-Train" (**Fig. 1(a)**), aerodynamically levitated by the Wing-In-Ground (WIG) effect [4]. In WIG phenomenon, the lift-drag ratio is increased by an air cushion effect between wing and the ground when the wing is near the ground or water. The Aero-Train is levitated based on this effect on a U-shaped guideway. This has several advantages over other systems – wind drag between the vehicle and guideway is lower than that in a magnetically levitated (MAGLEV) train and it is safer and more efficient than a WIG craft on water [5–8] because Aero-Train operation is based on the use of a solid guideway. Kohama et al. studied the height and lift-drag ratio strongly affected by the WIG effect and the effectiveness of a tandem wing configuration [9–12]. Actual levitated running of a prototype has been also achieved (**Fig. 1(b)**).

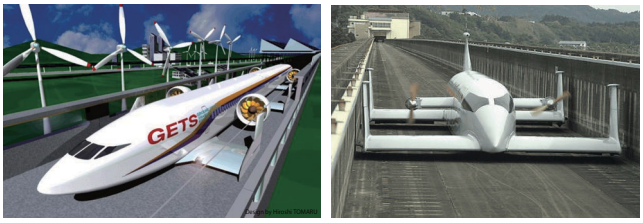

(a) Concept image [3]. (b) ART002 prototype [13].

Fig. 1. Aero-Train.

In an example of Aero-Train levitation control, levitated running was realized by simple PD control [14] and PID control [13] based on the distance measured between the ground and vehicle. However, their results are instable because the control methods were not based on a dynamic model of the WIG vehicle.

In a first step toward developing levitation control for the Aero-Train, we developed a small, lightweight, safe experimental WIG vehicle that levitates at low speed [15]. The U-shaped guideway used in ART002 experiments is large and we could not find a more appropriate guideway, so experiments are done on the airstrip of a gliding field without guide walls and our prototype has no guide wings. A dynamic model assuming that yaw and sideslip angles are negligible is derived, and control of position along the *Z* axis and orientation about the roll and pitch axes using a state feedback through a linear quadratic regulator is developed. Experiments confirmed the effectiveness of the

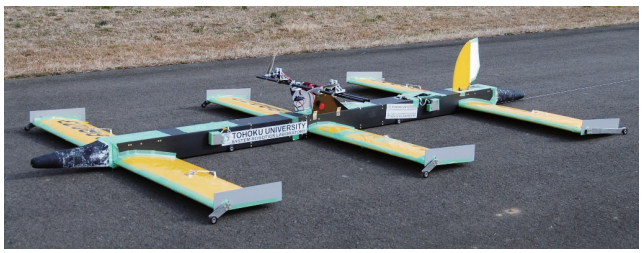

Fig. 2. Experimental WIG effect vehicle ARTE01 [15].

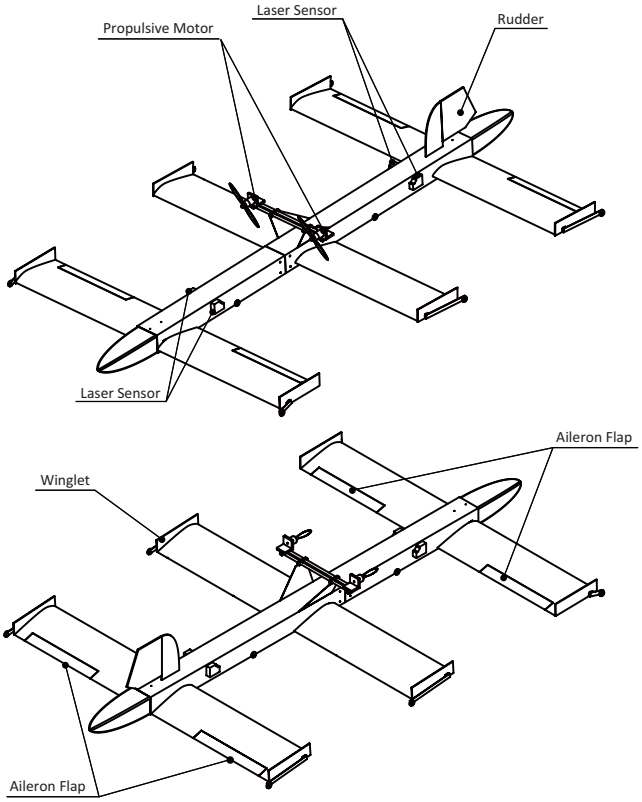

Fig. 3. Isometric view of ARTE01.

control developed.

A brief summary on the control and an experiment was described in [15]. This paper describes the detail of the developed experimental WIG vehicle prototype, modeling, control, simulations and several experimental results.

2. Experimental Ground Effect Vehicle

Figures 2–4 show the developed experimental WIG vehicle and **Table 1** lists specifications. Based on knowledge from studies on Aero-Train, experimental model ARTE01 was designed with the following features:

- Three levitation wings enabling levitation at low speed.
- Clark Y, effective in the ground effect, used as an airfoil.
- Winglets on the wingtips.

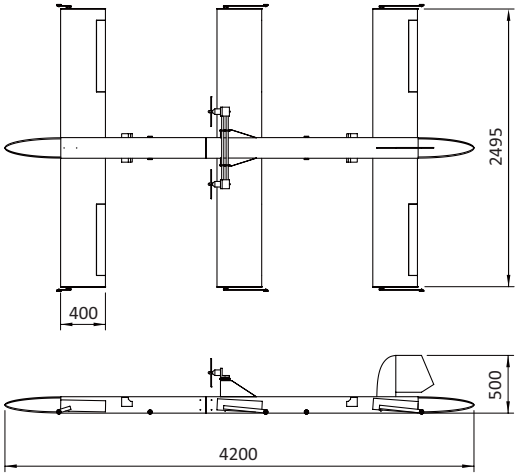

Fig. 4. Orthographic views of ARTE01.

Table 1. Specifications.

Model No.	ARTE01
Dimension / Weight	
Height	500 mm
Width	2495 mm
Length	4200 mm
Weight	20 kg
Wing	
Wing number	3
Airfoil	Clark Y
Chord length	400 mm
Wing span	2400 mm
Angle of attack (front)	2 deg
Angle of attack (mid)	4 deg
Angle of attack (rear)	5 deg
Moving blade	
Aileron flap	4
Rudder	1 (manual)
Thruster	
Number	2 (manual)
Model No.	E-flite 670Kv
Actuator	
Number	4
Model No.	SPAC-5-100-0003-SP168
Rated power	5 W
Maximum torque	2.7 Nm
Maximum speed	90 rpm
Computer / Electric System	
Computer	PC104
Displacement meter	ILD1401-200 x4

- Distances between levitation wings over 2.5 times the chord length.

Experiments are done on the ground without a guide wall, so only vehicle height and orientation about the roll and pitch axes are controlled. ARTE01 does not have guide wings or sensors to measure its location along longitudinal and lateral axes or yaw orientation.

Aileron flap control at the front and rear levitation wings driven by DC servomotors enables ARTE01 to levitate stably. This control is based on roll and pitch orientation angle error and height error computed from the distance between the ground and parts of the vehicle, measured by 4 laser displacement meters. Thrust from 2 propellers driven by motors and a rudder is operated manually via radio control signal to keep travel straight. Levitation wings are cannibalized from commercialized model aircrafts.

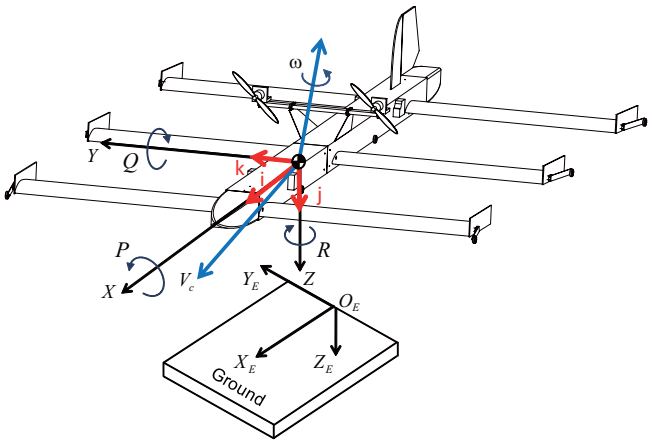

Fig. 5. Coordinate systems [15].

3. Dynamic Model

Figure 5 shows the coordinate systems used to model the experimental WIG vehicle. Vehicle coordinate system $O-XYZ$ is right-hand orthogonal and fixed on the vehicle. Its origin is fixed on the vehicle's center of gravity, and the X axis fits the vehicle velocity vector when the vehicle is in steady horizontal flight. World coordinate system $O_E-X_EY_EZ_E$ is right-hand orthogonal and fixed on the ground, and its X_E axis also fits the vehicle velocity vector in steady horizontal flight.

3.1. Disturbance Equation

The equation of motion of aircraft is generally written as follows [16]:

$$\begin{aligned} m(\dot{v}_x + qV_{z0}) &= -mg\theta\cos\theta_0 + \Delta X_a \\ m(\dot{v}_y + rV_{x0} - pV_{z0}) &= mg\cos\theta_0\phi + \Delta Y_a \\ m(\dot{v}_z - qV_{x0}) &= -mg\theta\sin\theta_0 + \Delta Z_a \end{aligned} \quad \ldots (1)$$

$$\begin{aligned} I_x\dot{p} - I_{xz}\dot{r} &= \Delta L_a \\ I_y\dot{q} &= \Delta M_a \\ -I_{xz}\dot{p} + I_z\dot{r} &= \Delta N_a \end{aligned} \quad \ldots (2)$$

$$\begin{aligned} \dot{\phi} &= p + r\tan\theta_0 \\ \dot{\theta} &= q \\ \dot{\psi} &= r\sec\theta_0 \end{aligned} \quad \ldots (3)$$

where m is vehicle mass; v_x, v_y and v_z are small variations in velocity along the X, Y, and Z axes; p, q, and r are small angular velocities about the roll, pitch, and yaw axes; V_{x0} and V_{z0} are velocities along the X and Z axes in steady horizontal flight; g is gravity acceleration; ϕ, θ, and ψ are roll, pitch and yaw angles; θ_0 is the pitch angle in steady horizontal flight; ΔX_a, ΔY_a, and ΔZ_a are variations in aerodynamic force along the X, Y, and Z axes; I_x, I_y, and I_z are moments of inertia about the X, Y, and Z axes; I_{xz} is product of inertia about the XZ plane; and ΔL_a, ΔM_a, and ΔN_a are small variations in aerodynamic moment about the roll, pitch, and yaw axes.

The vehicle velocity vector in steady horizontal flight fits the vehicle's X axis, so $\theta_0 = 0$ and $V_{z0} = 0$.

By introducing angle of attack $\alpha = v_z/V_{x0}$ and angle of sideslip $\beta = v_y/V_{x0}$, we assume that aerodynamic force and moment are functions of small disturbances v_x, p, q, r, α, β, aileron flap angles of the left front levitation wing δ_{flaf}, right front levitation wing δ_{fraf}, left rear levitation wing δ_{rlaf}, and right rear levitation wing δ_{rraf}, and the rudder angles of front vertical wing δ_{frd} and rear vertical wing δ_{rrd}, and the height of the vehicle from ground h. By expanding to a Taylor series and using the first terms, force and moment are written as follows:

$$\Delta X_a = \frac{\partial X_a}{\partial v_x}v_x + \frac{1}{V_{x0}}\frac{\partial X_a}{\partial \alpha}\alpha \quad \ldots (4)$$

$$\begin{aligned} \Delta Y_a = {} & \frac{1}{V_{x0}}\frac{\partial Y_a}{\partial \beta}\beta + \frac{\partial Y_a}{\partial p}p + \frac{\partial Y_a}{\partial r}r \\ & + \frac{\partial Y_a}{\partial \delta_{frd}}\delta_{frd} + \frac{\partial Y_a}{\partial \delta_{rrd}}\delta_{rrd} \end{aligned} \quad \ldots (5)$$

$$\begin{aligned} \Delta Z_a = {} & \frac{\partial Z_a}{\partial v_x}v_x + \frac{1}{V_{x0}}\frac{\partial Z_a}{\partial \alpha}\alpha + \frac{\partial Z_a}{\partial q}q + \frac{\partial Z_a}{\partial h}h \\ & + \frac{\partial Z_a}{\partial \delta_{fraf}}\delta_{fraf} + \frac{\partial Z_a}{\partial \delta_{flaf}}\delta_{flaf} \\ & + \frac{\partial Z_a}{\partial \delta_{rraf}}\delta_{rraf} + \frac{\partial Z_a}{\partial \delta_{rlaf}}\delta_{rlaf} \end{aligned} \quad \ldots (6)$$

$$\begin{aligned} \Delta L_a = {} & \frac{1}{V_{x0}}\frac{\partial L_a}{\partial \beta}\beta + \frac{\partial L_a}{\partial p}p + \frac{\partial L_a}{\partial r}r + \frac{\partial L_a}{\partial \delta_{fraf}}\delta_{fraf} \\ & + \frac{\partial L_a}{\partial \delta_{flaf}}\delta_{flaf} + \frac{\partial L_a}{\partial \delta_{rraf}}\delta_{rraf} + \frac{\partial L_a}{\partial \delta_{rlaf}}\delta_{rlaf} \\ & + \frac{\partial L_a}{\partial \delta_{frd}}\delta_{frd} + \frac{\partial L_a}{\partial \delta_{rrd}}\delta_{rrd} \end{aligned} \quad \ldots (7)$$

$$\begin{aligned} \Delta M_a = {} & \frac{\partial M_a}{\partial v_x}v_x + \frac{1}{V_{x0}}\frac{\partial M_a}{\partial \alpha}\alpha + \frac{\partial M_a}{\partial q}q \\ & + \frac{\partial M_a}{\partial h}h + \frac{\partial M_a}{\partial \delta_{fraf}}\delta_{fraf} + \frac{\partial M_a}{\partial \delta_{flaf}}\delta_{flaf} \\ & + \frac{\partial M_a}{\partial \delta_{rraf}}\delta_{rraf} + \frac{\partial M_a}{\partial \delta_{rlaf}}\delta_{rlaf} \end{aligned} \quad \ldots (8)$$

$$\begin{aligned} \Delta N_a = {} & \frac{1}{V_{x0}}\frac{\partial N_a}{\partial \beta}\beta + \frac{\partial N_a}{\partial p}p + \frac{\partial N_a}{\partial r}r + \frac{\partial N_a}{\partial \delta_{fraf}}\delta_{fraf} \\ & + \frac{\partial N_a}{\partial \delta_{flaf}}\delta_{flaf} + \frac{\partial N_a}{\partial \delta_{rraf}}\delta_{rraf} + \frac{\partial N_a}{\partial \delta_{rlaf}}\delta_{rlaf} \\ & + \frac{\partial N_a}{\partial \delta_{frd}}\delta_{frd} + \frac{\partial N_a}{\partial \delta_{rrd}}\delta_{rrd} \end{aligned} \quad \ldots (9)$$

Although ARTE01 has no front vertical wing, δ_{frd} is included considering future expandability.

Substituting Eqs. (4)–(9) into Eqs. (1) and (2) yields the following linearized small disturbance equation of mo-

tion:

$$\frac{dv_x}{dt} = \frac{1}{m}\frac{\partial X_a}{\partial v_x}v_x + \frac{1}{V_{x0}}\frac{1}{m}\frac{\partial X_a}{\partial \alpha}\alpha - g\theta \quad \ldots\ldots (10)$$

$$\frac{d\beta}{dt} = \frac{1}{V_{x0}}\left\{\frac{1}{V_{x0}}\frac{1}{m}\frac{\partial Y_a}{\partial \beta}\beta - V_{x0}r + g\phi + \frac{1}{m}\frac{\partial Y_a}{\partial p}p + \frac{1}{m}\frac{\partial Y_a}{\partial r}r + \frac{1}{m}\frac{\partial Y_a}{\partial \delta_{frd}}\delta_{frd} + \frac{1}{m}\frac{\partial Y_a}{\partial \delta_{rrd}}\delta_{rrd}\right\} \quad (11)$$

$$\frac{d\alpha}{dt} = \frac{1}{V_{x0}}\left\{\frac{1}{m}\frac{\partial Z_a}{\partial v_x}v_x + \frac{1}{m}\frac{1}{V_{x0}}\frac{\partial Z_a}{\partial \alpha}\alpha + V_{x0}q + \frac{1}{m}\frac{\partial Z_a}{\partial q}q + \frac{1}{m}\frac{\partial Z_a}{\partial h}h + \frac{1}{m}\left(\frac{\partial Z_a}{\partial \delta_{fraf}}\delta_{fraf} + \frac{\partial Z_a}{\partial \delta_{flaf}}\delta_{flaf} + \frac{\partial Z_a}{\partial \delta_{rraf}}\delta_{rraf} + \frac{\partial Z_a}{\partial \delta_{rlaf}}\delta_{rlaf}\right)\right\} \quad \ldots\ldots (12)$$

$$\frac{dp}{dt} = \frac{I_xI_z}{I_xI_z - {I_{xz}}^2}\left\{\frac{1}{V_{x0}}\left(\frac{1}{I_x}\frac{\partial L_a}{\partial \beta} + \frac{I_{xz}}{I_x}\frac{1}{I_z}\frac{\partial N_a}{\partial \beta}\right)\beta + \left(\frac{1}{I_x}\frac{\partial L_a}{\partial p} + \frac{I_{xz}}{I_x}\frac{1}{I_z}\frac{\partial N_a}{\partial p}\right)p + \left(\frac{1}{I_x}\frac{\partial L_a}{\partial r} + \frac{I_{xz}}{I_x}\frac{1}{I_z}\frac{\partial N_a}{\partial r}\right)r + \left(\frac{1}{I_x}\frac{\partial L_a}{\partial \delta_{frd}} + \frac{I_{xz}}{I_x}\frac{1}{I_z}\frac{\partial N_a}{\partial \delta_{frd}}\right)\delta_{frd} + \left(\frac{1}{I_x}\frac{\partial L_a}{\partial \delta_{rrd}} + \frac{I_{xz}}{I_x}\frac{1}{I_z}\frac{\partial N_a}{\partial \delta_{rrd}}\right)\delta_{rrd} + \left(\frac{1}{I_x}\frac{\partial L_a}{\partial \delta_{fraf}} + \frac{I_{xz}}{I_x}\frac{1}{I_z}\frac{\partial N_a}{\partial \delta_{fraf}}\right)\delta_{fraf} + \left(\frac{1}{I_x}\frac{\partial L_a}{\partial \delta_{flaf}} + \frac{I_{xz}}{I_x}\frac{1}{I_z}\frac{\partial N_a}{\partial \delta_{flaf}}\right)\delta_{flaf} + \left(\frac{1}{I_x}\frac{\partial L_a}{\partial \delta_{rraf}} + \frac{I_{xz}}{I_x}\frac{1}{I_z}\frac{\partial N_a}{\partial \delta_{rraf}}\right)\delta_{rraf} + \left(\frac{1}{I_x}\frac{\partial L_a}{\partial \delta_{rlaf}} + \frac{I_{xz}}{I_x}\frac{1}{I_z}\frac{\partial N_a}{\partial \delta_{rlaf}}\right)\delta_{rlaf}\right\} \quad (13)$$

$$\frac{dq}{dt} = \frac{1}{I_y}\frac{\partial M_a}{\partial v_x}v_x + \frac{1}{V_{x0}}\frac{1}{I_y}\frac{\partial M_a}{\partial \alpha}\alpha + \frac{1}{I_y}\frac{\partial M_a}{\partial q}q + \frac{1}{I_y}\frac{\partial M_a}{\partial h}h + \frac{1}{I_y}\left\{\frac{\partial M_a}{\partial \delta_{fraf}}\delta_{fraf} + \frac{\partial M_a}{\partial \delta_{flaf}}\delta_{flaf} + \frac{\partial M_a}{\partial \delta_{rraf}}\delta_{rraf} + \frac{\partial M_a}{\partial \delta_{rlaf}}\delta_{rlaf}\right\} \quad \ldots\ldots (14)$$

$$\frac{dr}{dt} = \frac{I_xI_z}{I_xI_z - {I_{xz}}^2}\left\{\frac{1}{V_{x0}}\left(\frac{1}{I_z}\frac{\partial N_a}{\partial \beta} + \frac{I_{xz}}{I_z}\frac{1}{I_x}\frac{\partial L_a}{\partial \beta}\right)\beta + \left(\frac{1}{I_z}\frac{\partial N_a}{\partial p} + \frac{I_{xz}}{I_z}\frac{1}{I_x}\frac{\partial L_a}{\partial p}\right)p + \left(\frac{1}{I_z}\frac{\partial N_a}{\partial r} + \frac{I_{xz}}{I_z}\frac{1}{I_x}\frac{\partial L_a}{\partial r}\right)r + \left(\frac{1}{I_z}\frac{\partial N_a}{\partial \delta_{frd}} + \frac{I_{xz}}{I_z}\frac{1}{I_x}\frac{\partial L_a}{\partial \delta_{frd}}\right)\delta_{frd} + \left(\frac{1}{I_z}\frac{\partial N_a}{\partial \delta_{rrd}} + \frac{I_{xz}}{I_z}\frac{1}{I_x}\frac{\partial L_a}{\partial \delta_{rrd}}\right)\delta_{rrd} + \left(\frac{1}{I_v}\frac{\partial N_a}{\partial \delta_{fraf}} + \frac{I_{xz}}{I_z}\frac{1}{I_x}\frac{\partial L_a}{\partial \delta_{fraf}}\right)\delta_{fraf} + \left(\frac{1}{I_z}\frac{\partial N_a}{\partial \delta_{flaf}} + \frac{I_{xz}}{I_z}\frac{1}{I_x}\frac{\partial L_a}{\partial \delta_{flaf}}\right)\delta_{flaf} + \left(\frac{1}{I_z}\frac{\partial N_a}{\partial \delta_{rraf}} + \frac{I_{xz}}{I_z}\frac{1}{I_x}\frac{\partial L_a}{\partial \delta_{rraf}}\right)\delta_{rraf} + \left(\frac{1}{I_z}\frac{\partial N_a}{\partial \delta_{rlaf}} + \frac{I_{xz}}{I_z}\frac{1}{I_x}\frac{\partial L_a}{\partial \delta_{rlaf}}\right)\delta_{rlaf}\right\} \quad \ldots\ldots (15)$$

Here, motion about the roll and yaw axis is mutually coupled because β, r, δ_{frd}, and δ_{rrd} are included in dp/dt in Eq. (13). However, β, r, and ψ cannot be measured and this experimental vehicle cannot control rudder angles δ_{frd} and δ_{rrd}. In this study, these motions have been decoupled assuming that:

- Yaw angular velocity and angle of sideslip are small, contributing to roll moment only negligibly.
- The vertical wing is small and contribution of the rudder angle to roll moment is only negligible.

From these assumptions, Eq. (13) is decoupled as follows:

$$\frac{dp}{dt} = \frac{I_xI_z}{I_xI_z - {I_{xz}}^2}\left\{\left(\frac{1}{I_x}\frac{\partial L_a}{\partial p} + \frac{I_{xz}}{I_x}\frac{1}{I_z}\frac{\partial N_a}{\partial p}\right)p + \left(\frac{1}{I_x}\frac{\partial L_a}{\partial \delta_{fraf}} + \frac{I_{xz}}{I_x}\frac{1}{I_z}\frac{\partial N_a}{\partial \delta_{fraf}}\right)\delta_{fraf} + \left(\frac{1}{I_x}\frac{\partial L_a}{\partial \delta_{flaf}} + \frac{I_{xz}}{I_x}\frac{1}{I_z}\frac{\partial N_a}{\partial \delta_{flaf}}\right)\delta_{flaf} + \left(\frac{1}{I_x}\frac{\partial L_a}{\partial \delta_{rraf}} + \frac{I_{xz}}{I_x}\frac{1}{I_z}\frac{\partial N_a}{\partial \delta_{rraf}}\right)\delta_{rraf} + \left(\frac{1}{I_x}\frac{\partial L_a}{\partial \delta_{rlaf}} + \frac{I_{xz}}{I_x}\frac{1}{I_z}\frac{\partial N_a}{\partial \delta_{rlaf}}\right)\delta_{rlaf}\right\} \quad (16)$$

3.2. Stability Derivatives

Coefficients of terms of the variation of each of individual aerodynamic force and moment differentiated partially by individual disturbances in Eqs. (10)–(16), called "stability derivatives," usually written as $(\partial X_a)/(\partial v_x) = X_{v_x}$, are handled as constants under fixed flight conditions.

3.2.1. $X_{v_x}, X_\alpha, Z_\alpha, M_\alpha$

Stability derivatives X_{v_x}, X_α, Z_α, and M_α are written as follows [16]:

$$\frac{1}{m}\frac{\partial X_a}{\partial v_x} = -\frac{1}{m}\left(\frac{T_0}{V_{x0}} + \rho V_{x0}SC_D\right) \quad \ldots\ldots (17)$$

$$\frac{1}{m}\frac{\partial X_a}{\partial \alpha} = \frac{\rho {V_{x0}}^2 S}{2m}\frac{1 - 2C_{L\alpha}}{\pi eAR}C_L \quad \ldots\ldots (18)$$

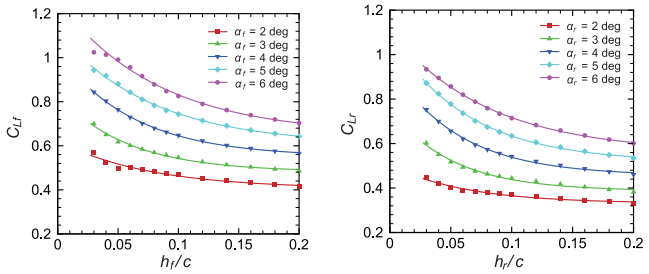

(a) Front wing. (b) Rear wing.

Fig. 6. Experimental results and fitted curve of lift coefficient [17].

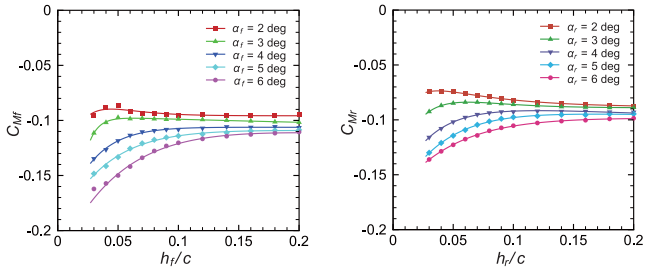

(a) Front wing. (b) Rear wing.

Fig. 7. Experimental results and fitted curve of moment coefficient [17].

$$\frac{1}{m}\frac{\partial Z_a}{\partial \alpha} = -\frac{\rho {V_{x0}}^2 S}{2m} C_{L\alpha} \quad \ldots\ldots\ldots (19)$$

$$\frac{1}{I_y}\frac{\partial M_a}{\partial \alpha} = -\frac{\rho {V_{x0}}^2 Sc}{2I_y} C_{m\alpha} \quad \ldots\ldots\ldots (20)$$

where T_0 is steady thrust, ρ is atmospheric density, S is levitation wing area, e is Oswald's airplane efficiency ($=0.6$), AR is the aspect ratio, C_D is the drag coefficient, C_L is the lift coefficient, $C_{L\alpha} = \partial C_L/\partial\alpha$ is the lift curve slope, $C_{m\alpha} = \partial C_m/\partial\alpha$ is the pitching moment curve slope, and C_m is the moment coefficient.

C_L, $C_{L\alpha}$, and $C_{m\alpha}$, in Eqs. (17)–(20), are under a strong WIG effect.

3.2.2. C_L

The lift coefficient of vehicle C_L is the sum of the lift coefficients of front, middle, and rear levitation wings C_{Lf}, C_{Lm}, and C_{Lr}:

$$C_L = C_{Lf} + C_{Lm} + C_{Lr}. \quad \ldots\ldots\ldots (21)$$

Honda [17] studied C_L under the WIG effect in wind tunnel experiments using a moving belt and reported that this affects the wing strongly when the wing's rear edge height from the ground is less than 20% of the chord length. In this region, lift and pitching moment coefficients vary nonlinearly, e.g., those of airfoil NACA6412-modified, similar to Clark Y, under the WIG effect from Honda's experimental study are shown in **Figs. 6** and **7**. Honda pointed out that the difference between front and rear wings is due to the after-flow from the front wing in

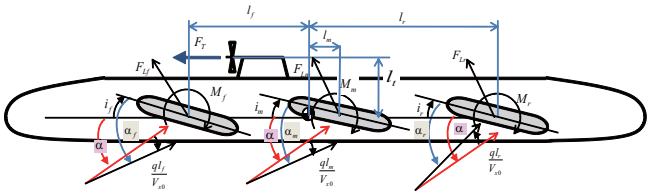

Fig. 8. Lift and pitching moment [15].

C_L of the rear wing. Eq. (22) is the modified equation for the fitted curve of **Fig. 6**, in which wing lift coefficients are the sum of the normal lift coefficient and terms of the WIG effect.

$$\begin{aligned}
C_{Lf} &= C_{Lfg.e} + C_{Lfnormal} \\
&= a_1 \exp\left(-a_2 \frac{h_f}{c}\right) + a_3\alpha_f + a_4 \\
&\quad + \frac{\partial C_{Lf}}{\partial \delta_{fraf}}\delta_{fraf} + \frac{\partial C_{Lf}}{\partial \delta_{flaf}}\delta_{flaf} \\
C_{Lm} &= C_{Lmg.e} + C_{Lmnormal} \\
&= b_1 \exp\left(-b_2 \frac{h_m}{c}\right) + b_3\alpha_m + b_4 \\
C_{Lr} &= C_{Lrg.e} + C_{Lrnormal} \\
&= b_1 \exp\left(-b_2 \frac{h_r}{c}\right) + b_3\alpha_r + b_4 \\
&\quad + \frac{\partial C_{Lr}}{\partial \delta_{rraf}}\delta_{rraf} + \frac{\partial C_{Lr}}{\partial \delta_{rlaf}}\delta_{rlaf} \quad \ldots\ldots (22)
\end{aligned}$$

where $C_{Lfg.e}$, $C_{Lmg.e}$, and $C_{Lrg.e}$ are lift coefficients for the WIG effect of the front, middle, and rear wings; $C_{Lfnormal}$, $C_{Lmnormal}$, and $C_{Lrnormal}$ are lift coefficients without the WIG; h_f, h_m, and h_r are heights of rear edges of the wing from the ground; c is the chord length; h_f/c, h_m/c, and h_r/c are height-chord ratios; and α_f, α_m, and α_r are angles of attack. a_1–a_3 and b_1–b_4 are parameters of the fitted curve obtained experimentally.

As shown in **Fig. 8**, angles of attack for each wing α_f, α_m, and α_r sum the angle of attack of vehicle α, mounting angles of each wing i_f, i_m, and i_r and apparent angles of attack caused by pitching angular velocity $-ql_f/V_{x0}$, ql_m/V_{x0}, and ql_r/V_{x0}. Heights of rear edges h_f, h_m, and h_r are sums of height and its variations from the pitch angle. This means that in a geometric relationship, these values are obtained from α, q, V_{x0}, θ, the height of the vehicle in steady horizontal flight h_0, and variations in height of vehicle h as follows:

$$\begin{aligned}
&\alpha_f = \alpha + i_f - \frac{ql_f}{V_{x0}}, \quad \alpha_m = \alpha + i_m + \frac{ql_m}{V_{x0}}, \\
&\alpha_r = \alpha + i_r + \frac{ql_r}{V_{x0}}, \quad h_f = h_0 + h + l_f\theta, \\
&h_m = h_0 + h + l_m\theta, \quad h_r = h_0 + h + l_r\theta. \quad . \quad (23)
\end{aligned}$$

Ishizuka [18] studied the variation of C_L by the aileron flap angle under the WIG using wind tunnel experiment and moving belt, reporting the proportional relationship between the aileron flap angle and the lift co-

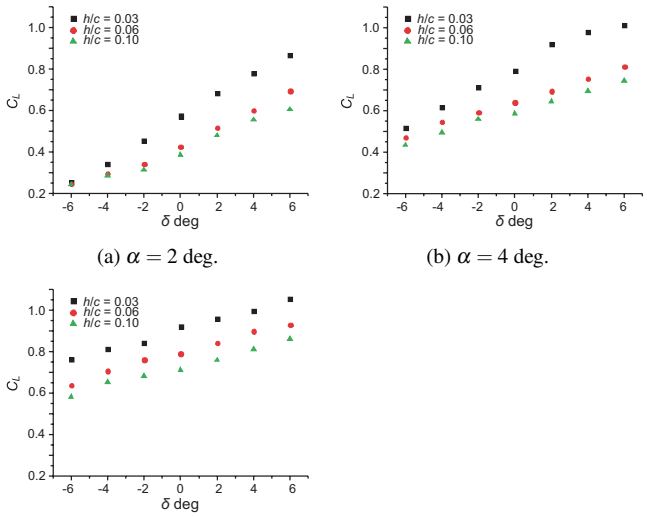

(a) $\alpha = 2$ deg. (b) $\alpha = 4$ deg.

(c) $\alpha = 6$ deg.

Fig. 9. Experimental results of lift coefficient [18].

efficient shown in **Fig. 9**. $\partial C_{Lf}/\partial\delta_{fraf}$, $\partial C_{Lf}/\partial\delta_{flaf}$, $\partial C_{Lr}/\partial\delta_{rraf}$, and $\partial C_{Lr}/\partial\delta_{rlaf}$ are obtained as linear functions.

3.2.3. $C_{L\alpha}$

By substituting Eqs. (22) and (23) into Eq. (21) and partially differentiating them by α, $\partial C_L/\partial\alpha$ is obtained as follows:

$$\frac{\partial C_L}{\partial\alpha} = a_3 + 2b_3. \quad \ldots\ldots\ldots\ldots (24)$$

3.2.4. $C_{m\alpha}$

Consider the pitching moment acting on the vehicle:

$$M = M_f + M_m + M_r + M_{fus} + l_f L_f - l_m L_m - l_r L_r - T l_t \quad \ldots\ldots (25)$$

where M_f, M_m, and M_r are moments generated by the front, middle, and rear levitation wings; M_{fus} is the moment generated by the vehicle; L_f, L_m, and L_r are lift generated by the front, middle, and rear levitation wings; and T is thrust.

The moment coefficient of the vehicle C_m is obtained by dividing Eq. (25) by $(1/2)\rho {V_{x0}}^2 Sc$ as follows:

$$C_m = C_{mf} + C_{mm} + C_{mr} + C_{mfus} + \frac{l_f}{c}C_{Lf} - \frac{l_m}{c}C_{Lm} - \frac{l_r}{c}C_{Lr} - \frac{T l_t}{(1/2)\rho V_{x0}^2 Sc} \quad (26)$$

where C_{mf}, C_{mm}, C_{mr}, and C_{mfus} are moment coefficients of the front, middle, and rear levitation wings, and the vehicle.

Here, as with the lift coefficient, wing moment coefficients sum the normal moment coefficient and terms of the WIG effect [17]. Eq. (27) is the fitted curve of **Fig. 7**:

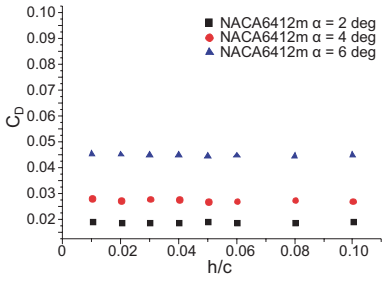

Fig. 10. Experimental results of drag coefficient [18].

$$\begin{aligned}
C_{mf} &= C_{mfg.e} + C_{mfnormal} \\
&= a_5 \exp\left(-a_6\frac{h_f}{c}\right) + a_7 \exp\left(-a_8\frac{h_f}{c}\right) \\
&\quad + a_9\alpha_f + a_{10} \\
C_{mm} &= C_{mmg.e} + C_{mmnormal} \\
&= b_5 \exp\left(-b_6\frac{h_m}{c}\right) + b_7 \exp\left(-b_8\frac{h_m}{c}\right) \\
&\quad + b_9\alpha_m + b_{10} \\
C_{mr} &= C_{mrg.e} + C_{mrnormal} \\
&= b_5 \exp\left(-b_6\frac{h_r}{c}\right) + b_7 \exp\left(-b_8\frac{h_r}{c}\right) \\
&\quad + b_9\alpha_r + b_{10} \quad \ldots\ldots\ldots\ldots (27)
\end{aligned}$$

where a_5–a_{10} and b_5–b_{10} are fitted curve parameters found experimentally.

C_{mfus} is computed as follows [16]:

$$C_{mfus} = \frac{2V_{fus}}{Sc}\alpha \quad \ldots\ldots\ldots\ldots (28)$$

where V_{fus} is the volume of the vehicle.

Substituting Eqs. (23), (27), and (28) into Eq. (26) and partially differentiating them by α yields $C_{m\alpha}$ as follows:

$$C_{m\alpha} = a_9 + 2b_9 + \frac{lf}{c}a_3 - \frac{l_m + l_r}{c}b3 + \frac{2V_{fus}}{Sc} \quad . (29)$$

3.2.5. C_D

As shown in **Fig. 10**, Ishizuka [18] reported that the WIG effect does not contribute to C_D, so C_D is a function only of the angle of attack easily be obtained from **Fig. 10**. This is why the WIG effect improves the lift-drag ratio.

3.2.6. Z_h

When the system is balanced, from the definition of the lift coefficient, Z_a is written as follows:

$$Z_a = -\frac{1}{2}\rho {V_{x0}}^2 S C_L \quad \ldots\ldots\ldots\ldots (30)$$

Considering Eqs. (21)–(23) and partially differentiating this by h yields the following equation:

$$\frac{1}{m}\frac{\partial Z_a}{\partial h} = \frac{\rho {V_{x0}}^2 S}{2mc}\left\{a_1 a_2 \exp\left(-\frac{a_2}{c}h_f\right) + b_1 b_2 \exp\left(-\frac{b_2}{c}h_m\right) + b_1 b_2 \exp\left(-\frac{b_2}{c}h_r\right)\right\} \quad (31)$$

3.2.7. M_h

In the same way, considering Eqs. (22), (23) and (26)–(28) and partially differentiating Eq. (25) by h yields the follow:

$$\begin{aligned}\frac{1}{I_y}\frac{\partial M_a}{\partial h} = -\frac{\rho {V_{x0}}^2 S}{2I_y}\Bigg\{ & a_5 a_6 \exp\left(-\frac{a_6}{c}h_f\right) \\ & + a_7 a_8 \exp\left(-\frac{a_8}{c}h_f\right) + b_5 b_6 \exp\left(-\frac{b_6}{c}h_m\right) \\ & + b_7 b_8 \exp\left(-\frac{b_8}{c}h_m\right) + b_5 b_6 \exp\left(-\frac{b_6}{c}h_r\right) \\ & + b_7 b_8 \exp\left(-\frac{b_8}{c}h_r\right) + \frac{l_f}{c} a_1 a_2 \exp\left(-\frac{a_2}{c}h_f\right) \\ & - \frac{l_m}{c} b_1 b_2 \exp\left(-\frac{b_2}{c}h_m\right) \\ & - \frac{l_r}{c} b_1 b_2 \exp\left(-\frac{b_2}{c}h_r\right)\Bigg\}. \quad \ldots\ldots (32)\end{aligned}$$

3.2.8. $Z_{\delta_{fraf}}, Z_{\delta_{flaf}}, Z_{\delta_{rraf}}, Z_{\delta_{rlaf}}$

On normal aircraft, stability derivative Z_{δ_e}, a derivative of Z_a with respect to a small disturbance in aileron angle δ_e, is usually written as follows [16]:

$$\begin{aligned}\frac{1}{m}\frac{\partial Z_a}{\partial \delta_e} &= \frac{\rho {V_{x0}}^2 S}{2m} C_{z_{\delta e}} \\ C_{z_{\delta e}} &= -\frac{\partial C_L}{\partial \delta_e}. \quad \ldots\ldots\ldots\ldots (33)\end{aligned}$$

In the same way, using Eqs. (21) and (22), $Z_{\delta_{fraf}}$, $Z_{\delta_{flaf}}$, $Z_{\delta_{rraf}}$, and $Z_{\delta_{rlaf}}$ are obtained as follows:

$$\begin{aligned}\frac{1}{m}\frac{\partial Z_a}{\partial \delta_{fraf}} &= -\frac{\rho {V_{x0}}^2 S}{2m}\frac{\partial C_{Lf}}{\partial \delta_{fraf}} \\ \frac{1}{m}\frac{\partial Z_a}{\partial \delta_{flaf}} &= -\frac{\rho {V_{x0}}^2 S}{2m}\frac{\partial C_{Lf}}{\partial \delta_{flaf}} \\ \frac{1}{m}\frac{\partial Z_a}{\partial \delta_{rraf}} &= -\frac{\rho {V_{x0}}^2 S}{2m}\frac{\partial C_{Lr}}{\partial \delta_{rraf}} \\ \frac{1}{m}\frac{\partial Z_a}{\partial \delta_{rlaf}} &= -\frac{\rho {V_{x0}}^2 S}{2m}\frac{\partial C_{Lr}}{\partial \delta_{rlaf}}. \quad \ldots\ldots (34)\end{aligned}$$

As stated, $\partial C_{Lf}/\partial \delta_{fraf}$, $\partial C_{Lf}/\partial \delta_{flaf}$, $\partial C_{Lr}/\partial \delta_{rraf}$, and $\partial C_{Lr}/\partial \delta_{rlaf}$ are experimentally obtained as constants.

3.2.9. $M_{\delta_{fraf}}, M_{\delta_{flaf}}, M_{\delta_{rraf}}, M_{\delta_{rlaf}}$

As with $Z_{\delta e}$, on normal aircraft, stability derivative M_{δ_e}, a derivative of M_a with respect to a small disturbance in aileron angle δ_e, is obtained as follows [16]:

$$\begin{aligned}\frac{1}{I_y}\frac{\partial M_a}{\partial \delta_e} &= \frac{\rho {V_{x0}}^2 S\bar{c}}{2I_y} C_{m_{\delta e}} \\ C_{m_{\delta e}} &= \frac{\partial C_m}{\partial \delta_e}. \quad \ldots\ldots\ldots (35)\end{aligned}$$

Using Eqs. (22), (23), (25)–(28), $M_{\delta_{fraf}}$, $M_{\delta_{flaf}}$, $M_{\delta_{rraf}}$, and $M_{\delta_{rlaf}}$ are obtained as follows:

$$\begin{aligned}\frac{1}{m}\frac{\partial M_a}{\partial \delta_{fraf}} &= \frac{\rho {V_{x0}}^2 S l_f}{2I_y}\frac{\partial C_{Lf}}{\partial \delta_{fraf}} \\ \frac{1}{m}\frac{\partial M_a}{\partial \delta_{flaf}} &= \frac{\rho {V_{x0}}^2 S l_f}{2I_y}\frac{\partial C_{Lf}}{\partial \delta_{flaf}} \\ \frac{1}{m}\frac{\partial M_a}{\partial \delta_{rraf}} &= -\frac{\rho {V_{x0}}^2 S l_r}{2I_y}\frac{\partial C_{Lr}}{\partial \delta_{rraf}} \\ \frac{1}{m}\frac{\partial M_a}{\partial \delta_{rlaf}} &= -\frac{\rho {V_{x0}}^2 S l_r}{2I_y}\frac{\partial C_{Lr}}{\partial \delta_{rlaf}}. \quad \ldots\ldots (36)\end{aligned}$$

3.3. State Space Equation

From the above, the following state space equation is obtained:

$$\begin{aligned}\frac{d\mathbf{x}}{dt} &= \mathbf{A}\mathbf{x} + \mathbf{B}\mathbf{u} \\ \mathbf{y} &= \mathbf{C}\mathbf{x} \quad \ldots\ldots\ldots\ldots\ldots (37)\end{aligned}$$

$$\begin{aligned}\mathbf{x} &= \begin{bmatrix} v_x & \alpha & q & \theta & h & p & \phi \end{bmatrix}^T \\ \mathbf{u} &= \begin{bmatrix} \delta_{fraf} & \delta_{flaf} & \delta_{rraf} & \delta_{rlaf} \end{bmatrix}^T \\ \mathbf{y} &= \begin{bmatrix} \theta & h & \phi \end{bmatrix}^T \quad \ldots\ldots\ldots\ldots (38)\end{aligned}$$

$$\mathbf{A} = \begin{bmatrix} \frac{1}{m}\frac{\partial X_a}{\partial v_x} & \frac{1}{V_{x0}}\frac{1}{m}\frac{\partial X_a}{\partial \alpha} & 0 & -g & 0 & 0 & 0 \\ \frac{1}{V_{x0}m}\frac{\partial Z_a}{\partial v_x} & \frac{1}{{V_{x0}}^2 m}\frac{\partial Z_a}{\partial \alpha} & 1+\frac{1}{V_{x0}m}\frac{\partial Z_a}{\partial q} & 0 & \frac{1}{V_{x0}m}\frac{\partial Z_a}{\partial h} & 0 & 0 \\ \frac{1}{I_y}\frac{\partial M_a}{\partial v_x} & \frac{1}{V_{x0}}\frac{1}{I_y}\frac{\partial M_a}{\partial \alpha} & \frac{1}{I_y}\frac{\partial M_a}{\partial q} & 0 & \frac{1}{I_y}\frac{\partial M_a}{\partial h} & 0 & 0 \\ 0 & 0 & 1 & 0 & 0 & 0 & 0 \\ 0 & -V_{x0} & 0 & V_{x0} & 0 & 0 & 0 \\ 0 & 0 & 0 & 0 & 0 & I'\frac{\partial L_a}{\partial p} + I\frac{\partial N_a}{\partial p} & 0 \\ 0 & 0 & 0 & 0 & 0 & 1 & 0 \end{bmatrix} \quad \ldots\ldots (39)$$

$$\mathbf{B} = \begin{bmatrix} 0 & 0 & 0 & 0 \\ \frac{1}{V_{x0}}\frac{1}{m}\frac{\partial Z_a}{\partial \delta_{fraf}} & \frac{1}{V_{x0}}\frac{1}{m}\frac{\partial Z_a}{\partial \delta_{flaf}} & \frac{1}{V_{x0}}\frac{1}{m}\frac{\partial Z_a}{\partial \delta_{rraf}} & \frac{1}{V_{x0}}\frac{1}{m}\frac{\partial Z_a}{\partial \delta_{rlaf}} \\ \frac{1}{I_y}\frac{\partial M_a}{\partial \delta_{fraf}} & \frac{1}{I_y}\frac{\partial M_a}{\partial \delta_{flaf}} & \frac{1}{I_y}\frac{\partial M_a}{\partial \delta_{rraf}} & \frac{1}{I_y}\frac{\partial M_a}{\partial \delta_{rlaf}} \\ 0 & 0 & 0 & 0 \\ 0 & 0 & 0 & 0 \\ I'\frac{\partial L_a}{\partial \delta_{fraf}} + I\frac{\partial N_a}{\partial \delta_{fraf}} & I'\frac{\partial L_a}{\partial \delta_{flaf}} + I\frac{\partial N_a}{\partial \delta_{flaf}} & I'\frac{\partial L_a}{\partial \delta_{rraf}} + I\frac{\partial N_a}{\partial \delta_{rraf}} & I'\frac{\partial L_a}{\partial \delta_{rlaf}} + I\frac{\partial N_a}{\partial \delta_{rlaf}} \\ 0 & 0 & 0 & 0 \end{bmatrix} \quad \ldots\ldots (40)$$

$$\mathbf{C} = \begin{bmatrix} 0 & 0 & 0 & 1 & 0 & 0 & 0 \\ 0 & 0 & 0 & 0 & 1 & 0 & 0 \\ 0 & 0 & 0 & 0 & 0 & 0 & 1 \end{bmatrix} \quad \ldots\ldots (41)$$

where $I = I_{xz}/(I_x I_z - {I_{xz}}^2)$ and $I' = I_z/(I_x I_z - {I_{xz}}^2)$.

Here, all stability derivatives are assumed to be constants under steady horizontal flight conditions. Derivatives related to WIG effect, although strongly nonlinear, are also handled as constants when appropriate levitation height is assumed. Our future work includes controller design to use their nonlinearity effectively.

Note that roll and pitch are coupled via aileron flap effects, although they are usually decoupled in normal aircraft dynamics [16].

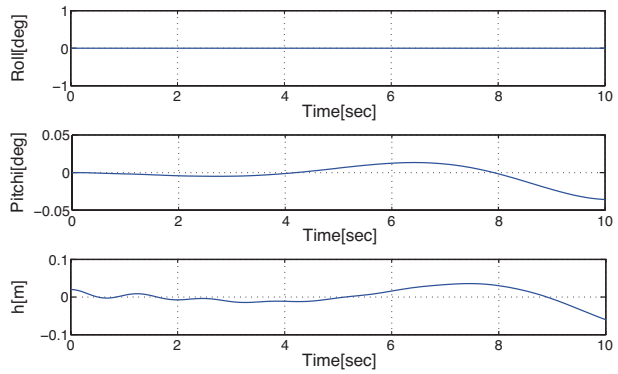

Fig. 11. Simulation results of initial h disturbance.

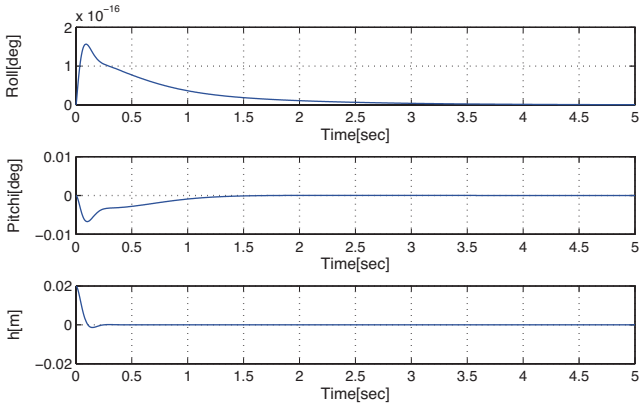

Fig. 12. Simulation results of initial h disturbance with control.

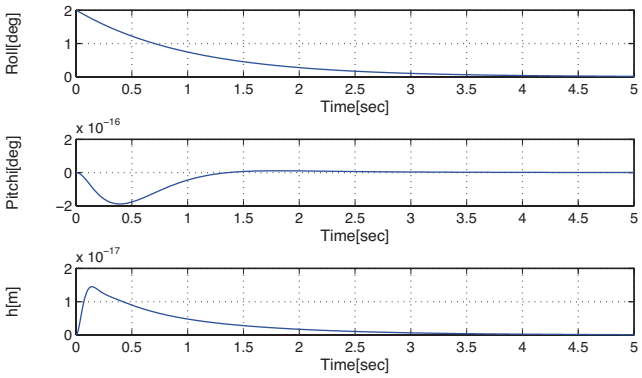

Fig. 13. Simulation results of initial ϕ disturbance with control.

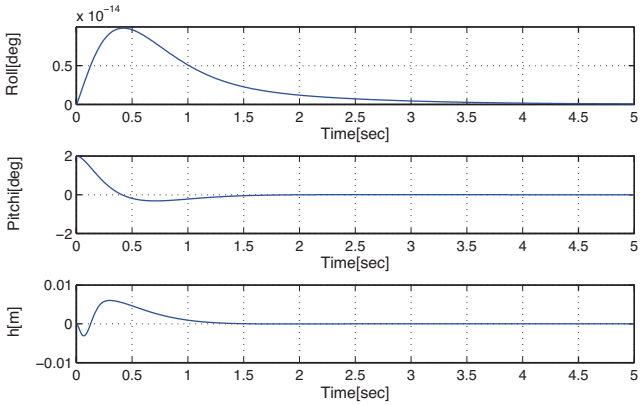

Fig. 14. Simulation results of initial θ disturbance with control.

4. Controller Design

Checking the eigenvalue of **A** and controllability matrix of the system shows that this system is unstable but controllable. **Fig. 11** shows simulation results with an initial disturbance of small vehicle height without control, indicating that vehicle height and pitch angle have diverged.

State feedback through the linear quadratic regulator was thus used as the controller. Weighting matrices were decided based on the movable ranges of aileron flaps as follows:

$$\mathbf{Q} = diag[50,50,50,50,500000,50,50]$$
$$\mathbf{R} = diag[1,1,1,1]. \quad \ldots\ldots\ldots \quad (42)$$

Simulations with initial disturbances of vehicle height, roll, and pitch angle were conducted using this controller, resulting in initial height disturbance of 0.02 m, roll disturbance of 2°, and pitch disturbance of 2° are shown in **Figs. 12–14**. Small roll errors occur in regulating pitch and height disturbances because longitudinal and lateral motions are coupled. Simulation results show that the vehicle height and roll and pitch angles converged at 0.

5. Experiments

To confirm the effectiveness of the experimental WIG vehicle ARTE01 and its controller, several levitation running experiments were conducted at the Kakuda glider field at Kakuda, Miyagi, Japan.

Figure 15 shows levitation running experiment results without control by fixing all aileron flaps. As is simulation results, vehicle height and pitch angle diverged. An appropriate controller is thus essential to have the WIG vehicle levitate stably.

In running experiments using the controller, desired levitation heights were set at 0.05 m ($h_0/c = 0.125$) and 0.1 m ($h_0/c = 0.25$), while desired roll and pitch angles were set at 0°.

Figure 16 shows levitation running experiment at a desired vehicle height of 0.05 m, with vehicle height and roll and pitch angle results shown in **Fig. 17**. Levitation started at 65 s. **Fig. 17** shows that although small vibrations occurred, vehicle height was generally 0.05 m and the pitch angle stabilized near 0° without undesirable pitching-up. Although the roll angle showed larger vibration with a maximum amplitude of 2°, it avoided divergence. Stable levitation with the desired vehicle height was thus realized using our proposed controller.

Figures 18 and **19** show levitation running experiment at a desired vehicle height of 0.1 m. Levitation starts at 63 s. Vehicle height rarely reached 0.1 m and error in orientation was larger than that at a desired vehicle height of 0.05 m, presumably because the WIG effect contribution to lift was reduced and it was difficult to obtain enough lift to stabilize orientation by controlling aileron flaps. De-

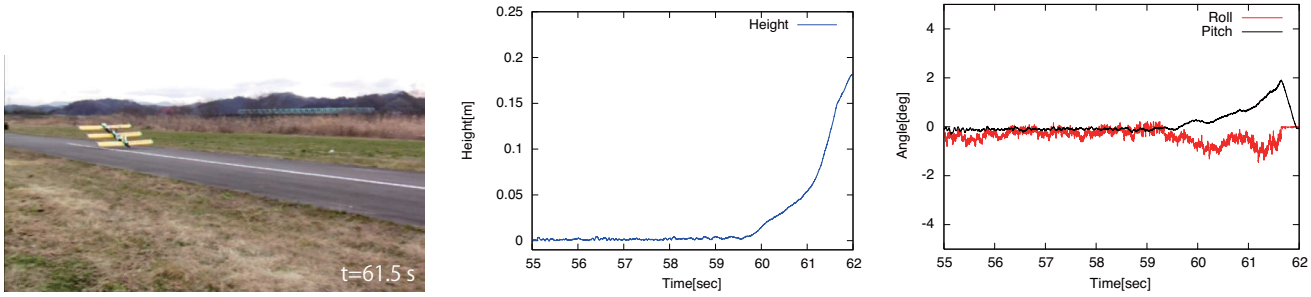

(a) Snapshot. (b) Height. (c) Roll, Pitch.

Fig. 15. Experimental results without control.

Fig. 16. Experiment of $h_0 = 0.05$ m.

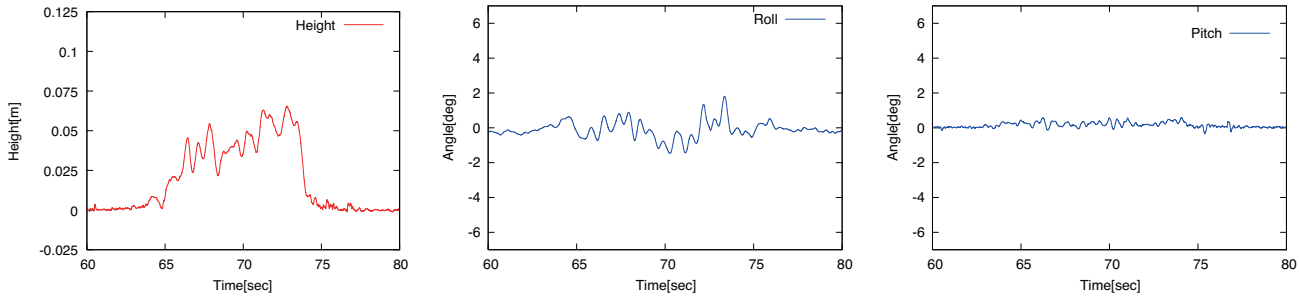

(a) Height. (b) Roll. (c) Pitch.

Fig. 17. Experimental results of $h_0 = 0.05$ m.

Fig. 18. Experiment of $h_0 = 0.10$ m.

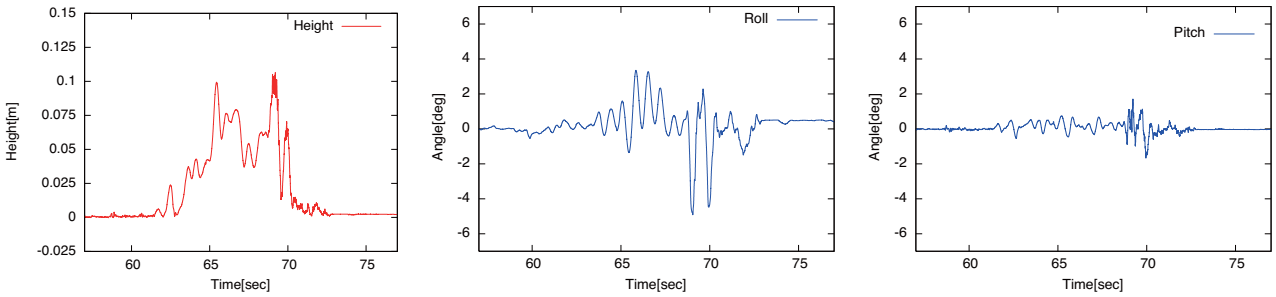

(a) Height. (b) Roll. (c) Pitch.

Fig. 19. Experimental results of $h_0 = 0.10$ m.

Fig. 20. Third prototype Aero-Train: manned experimental WIG vehicle ART003R.

signing an effective levitation height to use the WIG effect is thus also important in levitation control of the WIG vehicle.

6. Conclusions and Future Work

This paper has described the development, modeling, and controller of an experimental WIG vehicle. In the first development step of levitation control for Aero-Train, a small, lightweight experimental WIG vehicle that levitates at low speed was developed. The dynamic model in which the WIG is accounted for was derived and, by using this model, control based on a linear quadratic regulator was developed to stabilize the position along the Z axis and orientation about roll and pitch axes. Results of several experiments confirmed the effectiveness of the control developed.

In this study, the lateral position and yaw angle of the experimental vehicle could not be measured, so motions along roll and yaw axes were decoupled under several assumptions. The reasonableness of these assumptions is uncertain, however, and it was difficult to manually operate a rudder to keep vehicle travel straight. In our next report, we hope to develop a refined experimental WIG vehicle with guide wings and sensors to measure lateral and directional positions and a 6 DOF dynamic model and controller for stabilization along the Y and Z axes and around the roll, pitch, and yaw axes including control of running velocity on the U-shaped guideway.

The linearized disturbance equation must be improved. Even though C_L and C_m under the WIG are strongly nonlinear, all aerodynamic forces and moments have been finally linearized by treating all stability derivatives as constants. The effectiveness of this has been confirmed, but its reasonableness is questionable. We also plan to study the aerodynamic model including the nonlinear WIG and control based on the model.

Experiments for verifying high-speed control will be conducted using ART003R shown in **Fig. 20**, a manned experimental prototype still under development that travels at 200 km/h.

Acknowledgements

This work was done in part under the New Energy and Industrial Technology Development Organization (NEDO) Research and Development "Strategic Development of Energy Conservation Technology Project." We thank the many students who helped in the many experiments under harsh weather conditions.

References:

[1] Y. Kohama, "An Application of ACV to Railway Transportation," 25th Aircraft Symposium, pp. 128-131, 1987. (in Japanese)
[2] H. Tomaru and Y. Kohama, "Wind-Tunnel Investigation of Aerofoil for Wing in Ground Effect," Nagare, Vol.10, pp. 47-60, 1991. (in Japanese)
[3] Y. Kohama, "Mechanical Civilization Induced Earth Pollution Problem, and Aero-Train," Trans. of the Japan Society of Mechanical Engineers, Series B, Vol.71, No.707, pp. 1733-1737, 2005. (in Japanese)
[4] I. Tani, M. Taima, and S. Simidu, "The Effect of Ground on the Aerodynamic Characteristics of a Monoplane Wing," Report of the Aeronautical Research Institute, Tokyo Imperial University, Vol.13, No,156, pp. 22-76, 1937.
[5] R. G. Ollola, "Historical Review of WIG Vehicles," J. of HYDRONAUTICS, Vol.14, No.3, pp. 65-76, 1980.
[6] R. K. Nangia, "Aerodynamic and hydrodynamic aspects of high speed water surface craft," Aeronautical J., June/July, pp. 241-268, 1987.
[7] G. W. Jorg, "History and Development of the 'Aerodynamic Ground Effect craft' (AGEC) with Tandem Wings," Symp. Proc. Ram Wing and Ground-Effect Craft, Royal Aeronautical Society, pp. 87-109, 1987.
[8] K. V. Rozhdestvensky, "Wing-in-Ground Effect Vehicles," Progress in Aerospace Sciences, Vol.42, pp. 211-283, 2006.
[9] H. Tomaru and Y. Kohama, "Aerodynamics of Tandem-WIG in Guide Way," Nagare, Vol.11, pp. 45-52, 1992. (in Japanese)
[10] T. Kono, Y. Kohama, and N. Matsui, "Stability of Guide Way Type Wing in Ground Effect Vehicle," Proc. of the Third JSME-KSME Fluids Engineering Conf., pp. 715-718, 1994.
[11] Y. Kohama, T. Hikosaka, and H. Watanabe, "Experimental and Numerical Study of Aerodynamic Characteristics of a Ground Effect Transport System (GETS)," J. of the Japan Society for Aeronautical and Space Sciences Vol.47, No.541, pp. 79-87, 1999. (in Japanese)
[12] M. R. Ahmed and Y. Kohama, "Experimental Investigation on the Aerodynamic Characteristics of a Tandem Wing Configuration in Close Ground Proximity," JSME Int. J., Series B, Vol.42, No.4, pp. 612-618, 1999.
[13] S. Kikuchi, F. Ota, T. Kato, T. Ishikawa, and Y. Kohama, "Development of a Stability Control Method for the Aero-Train," J. of Fluid Science and Technology, Vol.2, No.1, pp. 226-237, 2007.
[14] Y. Kohama, H, Watanabe, S. Kikuchi, F. Ota, and T. Ito, "Flight Dynamics and Development of the Stability Control Method of the Aero-Train. 1st Report, Flight Test by Pushing," Trans. of the Japan Society of Mechanical Engineers, Series B, Vol.68, No.665, pp. 102-107, 2002. (in Japanese)
[15] Y. Sugahara, Y. Ikeuchi, R. Suzuki, Y. Hirata, K. Kosuge, Y. Noguchi, S. Kikuchi, and Y. Kohama, "Levitation Control of Experimental Wing-in-Ground Effect Vehicle along Z Axis and about Roll and Pitch Axes," Proc. of the 2011 IEEE Int. Conf. on Robotics and Automation, pp. 8-13, 2011.
[16] L. V. Schmidt, "Introduction to Aircraft Flight Dynamics," American Institute of Aeronautics and Astronautics, 1998.
[17] K. Honda, "Longitudinal Stability of WIG with Tandem Configuration," Master thesis, Tohoku University, 2002. (in Japanese)
[18] T. Ishizuka, "Aerodynamic Characteristics of Aerotrain Wings and Drag Reduction by Separation Control," Master thesis, Tohoku University, 2002. (in Japanese)

Name:
Yusuke Sugahara

Affiliation:
Assistant Professor, Department of Bioengineering and Robotics, Tohoku University

Address:
6-6-01 Aoba, Aramaki, Aoba-ku, Sendai 980-8579, Japan

Brief Biographical History:
2003-2006 Visiting Research Associate, Graduate School of Science and Engineering, Waseda University
2006 Received Ph.D. in Bioscience and Biomedical Engineering from Waseda University
2006-2007 Research Associate, Advanced Research Institute for Science and Engineering, Waseda University
2007- Assistant Professor, Department of Bioengineering and Robotics, Tohoku University

Main Works:
- "A Novel Stair-Climbing Wheelchair with Transformable Wheeled Four-Bar Linkages," Proc. of the 2010 IEEE/RSJ Int. Conf. on Intelligent Robots and Systems, pp. 3333-3339, 2010.
- "Walking Pattern Generation of Biped Walking Vehicle in Consideration of Passenger's Passive Dynamic Model," J. of the Robotics Society of Japan, Vol.25, No.6, pp. 842-850, 2007. (in Japanese)
- "Experimental Stiffness Measurement of WL-16RII Biped Walking Vehicle during Walking Operation," J. of Robotics and Mechatronics, Vol.19, No.3, pp. 272-280, 2007.

Membership in Academic Societies:
- The Japan Society of Mechanical Engineers (JSME)
- The Robotics Society of Japan (RSJ)
- Institute of Electrical and Electronics Engineers (IEEE)

Name:
Yusuke Ikeuchi

Affiliation:
Central Japan Railway Company

Address:
6-6-01 Aoba, Aramaki, Aoba-ku, Sendai 980-8579, Japan

Brief Biographical History:
2008 Received the B.E. from Tohoku University
2010 Received the M.E. from Tohoku University
2010- Central Japan Railway Company

Name:
Ryo Suzuki

Affiliation:
Mitsubishi UFJ Morgan Stanley Securities Co., Ltd.

Address:
6-6-01 Aoba, Aramaki, Aoba-ku, Sendai 980-8579, Japan

Brief Biographical History:
2010 Received the B.E. from Tokyo University of Science
2010- Mitsubishi UFJ Morgan Stanley Securities Co., Ltd.

Name:
Yasuhisa Hirata

Affiliation:
Associate Professor, Department of Bioengineering and Robotics, Tohoku University

Address:
6-6-01 Aoba, Aramaki, Aoba-ku, Sendai 980-8579, Japan

Brief Biographical History:
2000-2006 Research Associate, Department of Bioengineering and Robotics, Tohoku University
2002-2004 Researcher, JST PRESTO
2004 Received Ph.D. in Mechanical Engineering from Tohoku University
2006- Associate Professor, Department of Bioengineering and Robotics, Tohoku University

Main Works:
- "Transporting an Object by a Passive Mobile Robot with Servo Brakes in Cooperation with a Human," Advanced Robotics, Vol.23, No.4, pp. 387-404, 2009.
- "Motion Control of Passive Intelligent Walker Using Servo Brakes," IEEE Trans. on Robotics, Vol.23, No.5, pp. 981-990, 2007.
- "Coordinated Transportation of a Single Object by Omni-Directional Mobile Robots with Body Force Sensor," J. of Robotics and Mechatronics, Vol.12, No.3, pp. 242-248, 2000.

Membership in Academic Societies:
- The Japan Society of Mechanical Engineers (JSME)
- The Robotics Society of Japan (RSJ)
- The Society of Instrument and Control Engineers (SICE)
- Institute of Electrical and Electronics Engineers (IEEE)

Name:
Kazuhiro Kosuge

Affiliation:
Professor, Department of Bioengineering and Robotics, Tohoku University

Address:
6-6-01 Aoba, Aramaki, Aoba-ku, Sendai 980-8579, Japan

Brief Biographical History:
1980-1982 Research Staff, Department of Production Engineering, DENSO Corporation
1982-1990 Research Associate, Department of Control Engineering, Tokyo Institute of Technology
1988 Received Ph.D. in Mechanical Engineering from Tokyo Institute of Technology
1989-1990 Visiting Scientist, Department of Mechanical Engineering, Massachusetts Institute of Technology
1990-1995 Associate Professor, Nagoya University
1995- Professor, Tohoku University
1998-2001 Vice President, IEEE Robotics and Automation Society
2008-2009 President Elect, IEEE Robotics and Automation Society
2010- President, IEEE Robotics and Automation Society

Main Works:
• "Dance Step Estimation Method Based on HMM for Dance Partner Robot," Trans. on Industrial Electronics, Vol.54, No.2, pp. 699-706, 2007.

Membership in Academic Societies:
• The Japan Society of Mechanical Engineers (JSME)
• The Robotics Society of Japan (RSJ)
• The Society of Instrument and Control Engineers (SICE)
• Institute of Electrical and Electronics Engineers (IEEE)

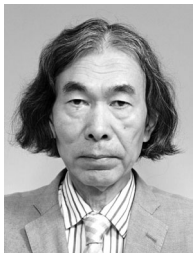

Name:
Yukio Noguchi

Affiliation:
Professor, Department of Industrial Management & Engineering, Faculty of Engineering, Tokyo University of Science

Address:
1-3 Kagurazaka, Shinjuku-ku, Tokyo 162-8601, Japan

Brief Biographical History:
1971-2002 Chief Researcher, Nippon Steel Corporation
1992 Received Ph.D. in Mechanical Engineering from Tokyo Institute of Technology
2002-2004 Professor, Department of Communication and Information Science, Fukushima National College of Technology
2004- Professor, Department of Industrial Management and Engineering, Tokyo University of Science

Main Works:
• "Multivariable Control of Bar Rolling and Precision Rolling System," J. of the Japan Society for Technology of Plasticity, Vol.42, No.480, pp. 70-74, 2001. (in Japanese)
• "Multivariable Control of Wire Rod Rolling Using Optimal Regulator Theory," Trans. of the Society of Instrument and Control Engineers, Vol.26, No.11, pp. 1283-1290, 1990. (in Japanese)

Membership in Academic Societies:
• The Japan Society for Technology of Plasticity (JSTP)
• The Japan Society of Mechanical Engineers (JSME)
• The Society of Instrument and Control Engineers (SICE)
• Institute of Electrical and Electronics Engineers (IEEE)

Name:
Satoshi Kikuchi

Affiliation:
Lecturer, Department of Mechanical and System Engineering, Gifu University

Address:
1-1 Yanagido, Gifu 501-1193, Japan

Brief Biographical History:
1999 Received Ph.D. in Mechanical Engineering from Tohoku University
1999-2004 Research Associate, Institute of Fluid Science, Tohoku University
2004- Lecturer, Department of Mechanical and System Engineering, Gifu University

Main Works:
• "Measurement of Ground Effect and Boundary-Layer Transition by Towing Wind Tunnel," Fluid Dynamics Research, Vol.41, No.2, 2009.
• "Development of a Stability Control Method for the Aero-Train," J. of Fluid Science and Technology, Vol.2, No.1, pp. 226-237, 2007.
• "Flow Characteristics of Plane Wall Jet with Side Walls on Both Sides," JSME Int. J., Series B, Vol.49, No.4, pp. 914-920, 2006.

Membership in Academic Societies:
• The Japan Society of Mechanical Engineers (JSME)
• The Japan Society of Fluid Mechanics (JSFM)

Name:
Yasuaki Kohama

Affiliation:
Professor, New Industry Creation Hatchery Center (NICHe), Tohoku University

Address:
6-6-10 Aoba, Aramaki, Aoba-ku, Sendai 980-8579, Japan

Brief Biographical History:
1974 Received Ph.D. in Mechanical Engineering from Tohoku University
1974-1981 Research Associate, Institute of High Speed Mechanics, Tohoku University
1981-1985 Lecturer, Institute of High Speed Mechanics, Tohoku University
1985-1996 Associate Professor, Institute of Fluid Science, Tohoku University
1996-2009 Professor, Institute of Fluid Science, Tohoku University
2009- Professor, New Industry Creation Hatchery Center (NICHe), Tohoku University

Main Works:
• "Measurement of Ground Effect and Boundary-Layer Transition by Towing Wind Tunnel," Fluid Dynamics Research, Vol.41, No.2, 2009.
• "Design Space Exploration of Supersonic Formation Flying Focusing on Drag Minimization," J. of Aircraft, Vol.45, No.2, pp. 430-439, 2008.
• "Development of a Stability Control Method for the Aero-Train," J. of Fluid Science and Technology, Vol.2, No.1, pp. 226-237, 2007.

Membership in Academic Societies:
• The Japan Society of Mechanical Engineers (JSME)
• The Japan Society of Fluid Mechanics (JSFM)
• The Japan Society for Aeronautical and Space Sciences (JSASS)
• American Physical Society (APS)